



Dynamic response of common stone masonry buildings under uncertain material properties

Rabindra Adhikari^{1,*}, Sanjita Gotame¹, Puja Regmi¹, Bipin Karki¹, Dipendra Gautam¹

¹ Department of Civil Engineering, Cosmos College of Management and Technology, Lalitpur, Nepal

*Corresponding email: rabindraadhikari@cosmoscollege.edu.np

Received: December 12, 2022; Revised: February 11, 2023; Accepted: February 13, 2023

doi:<https://doi.org/10.3126/joeis.v2i1.49592>

Abstract

The major causes of the failure of the structure are either improper design or improper construction. Therefore, accurate analysis for the design of the structure is of utmost importance. However, it is extremely difficult and impractical to determine all the engineering properties of the building structure and all of its components' analysis of each building. It is customary to adopt typical values of material properties for the analysis of such structures, usually required for seismic vulnerability analysis. However, there is a high variation in material characteristics, especially of stone masonry that can have a significant effect on the analysis. Typical stone masonry was investigated at the site and then analyzed using finite element model (FEM). Parametric analysis was conducted for a range of young's modulus of elasticity values of a masonry wall. The dynamic characteristics of the building were determined from the modal analysis. Seismic loading was done using dynamic methods and its effect was determined as design stresses and building deformations for the comparison. The results indicated that various building responses have a different relationship with the elasticity parameter of the wall, indicating that a very good engineering judgment is required in the analysis of stone masonry buildings that do not have standard material properties.

Keywords: building drifts, dynamic analysis, elasticity sensitivity of masonry buildings, seismic analysis; stone masonry

1. Introduction

Most of the stone buildings in Nepal do not fulfill architectural as well as structural standards and are highly vulnerable during earthquakes (Gautam, 2018; Gautam et al., 2016; Gautam & Chaulagain, 2016). Building codes (Nepal National Building Code for Seismic Design of Buildings in Nepal) including those governing the structural system of building (eg. NBC105, NBC202, etc.) have not been implemented in most parts of the country and thus the majority of the buildings do not meet seismic safety standards (Gautam & Chaulagain, 2016). In the few municipalities where the building code has been implemented from the last decade, the implementation is still at the preliminary stage and compliance is low (R. Adhikari et al., 2022). The country, therefore, is accumulating a large number of seismically vulnerable buildings every

year. Immediate attention to the safety of these buildings is of utmost importance, as moderate to strong earthquakes are deemed likely to occur throughout the country.

Stone masonry is the most prevalent typology of building in the rural area of Nepal (R. Adhikari & Gautam, 2019; Gautam et al., 2018, 2020). Recent earthquakes in Nepal and neighboring regions have revealed that stone masonry buildings are highly vulnerable during earthquakes (Ahmad et al., 2012; Chettri et al., 2021a, 2021b; Gautam et al., 2021, 2022). Further, the study of such structures has increased in recent years (see e. g. Varum et al., 2018), including several initiations in retrofitting of such structures either individually or by various governmental and non-governmental organizations.

However, the identification of various engineering parameters of construction materials and the system is challenging for masonry structures (R. Adhikari et al., 2019). For instance, young's modulus of elasticity of stone-masonry in mud mortar is dependent on various aspects such as the type of stone, source of mud for mortar, level of compaction of mortar, water content, porosity of the mortar, and the present dampness of the wall, among others. As most of the rural constructions are informally built with the available materials at the local level, these characteristics vary in a wide range. But, during most of the analysis and design of such structures, material properties are established by engineering judgment and rarely backed up with few test data. Further, such tests are often small in numbers and represent the information around the test area of the structure and may significantly vary on the other part of the structures (Adhikari et al., 2019; Parajuli, 2021; Parajuli et al., 2020; Parajuli & Kiyono, 2015). Hence, there is certain uncertainty in the current method of analysis of such masonry structures; the degree of such uncertainty is not well established.

This study investigates the effect of the change of properties of various construction materials commonly used in rural masonry building construction. The specific objectives of this study is to investigate the effect of variation of young's modulus of elasticity (and hence the stiffness) of the masonry wall on the structural response of the building such as natural period of the building, seismic base moments, design forces in masonry elements, storey displacements and building drifts.

2. Materials and Methods

2.1 Building description

A field visit was made to the rural hilly area of Nepal at Bhakundebesi of Kavre district, to document the construction system of a few mud mortar stone masonry residential buildings. A typical stone masonry building made of mud mortar as shown in Figure 1 was chosen for a detailed study that has about 462 square feet of floor area. Figure 2 shows the plan of the building (unspecified dimensions are mm) and Figure 3 shows the four side elevations of the building. Although most of the building have no openings on the back, and rare openings on the side, this particular building faces both front and back and has relatively large openings. Such type of building is found in hilly terrain in significant numbers, in relatively less steep terrain when the back side has no large hill and the terrain permits entry to the building. In this building, on the hill side, the wall is partially attached to soil upto about 600mm from the plinth level on the ground floor. Such case is more prominent in building in hilly area, when there is hill in backside of the building.



Figure 1: Front-view (left) and side-view (right) of the study building

Then the structure was studied for its response to changes in various material properties. The study has been conducted to a wide range of material properties to observe their effect on the structural response.

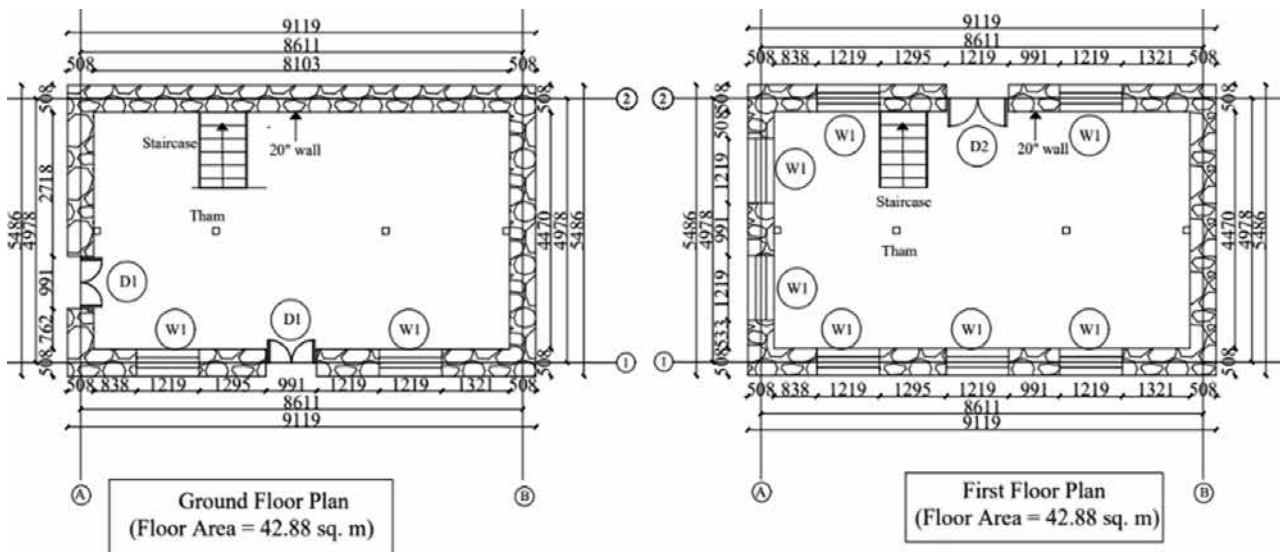


Figure 2: Plan of Building

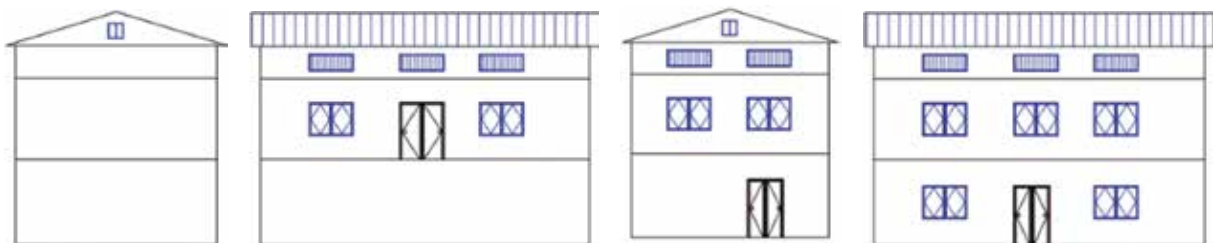


Figure 3: Left, front, right, and back elevation of the study building (left to right)

2.3 Finite element analysis

Finite element modeling was adopted for the detailed structural analysis of the buildings using ETABS v. 18 (Computers and Structures Inc., 2020). A three-dimensional finite element model (FEM) is shown in Figure 4. Walls were modeled as thick shell element while liner elements such as timber joists, Nidal (heaviest timber girder in the floor), Dalin (timber stinger beams supporting over the Nidal and peripheral walls), roof-rafters, and roof-purlins were modeled as frame elements. The loads on the floor were applied to the Dalin and the floor slab was not modeled, considering the fact that the floor has significantly small in-plane stiffness. Similarly, loads of roofing sheets were calculated and applied through the purlins. Loads in the cantilever portion of the roof were applied at the edge wall and purlins as applicable.

In this study, linear elastic analysis was conducted to evaluate the structural behavior of a building under the effects of dead loads, live loads, and earthquake loads. The dead and live loads were calculated according to IS 875 Part-I and Part-II respectively, while the earthquake loads were determined based on (NBC-105:2020 Nepal National Building Code for Seismic Design of Buildings in Nepal, 2020). Considering soft soil in the Kavre district, and considering unreinforced masonry, the base shear coefficient was calculated to be 0.53 with a base shear force of 1163KN. The base shear was distributed linearly over the height of the building according to the code provisions for low-period buildings. The design load combination was determined using the working stress method, as specified in NBC 105:1994 as such provision is not available in the latest version of the code, and the critical design forces were calculated as the envelope of all design load combinations for comparison purposes. As the characteristics of material in masonry buildings varies from building to building and in-situ test of the materials was not possible which is the usual case for small scale projects, typical properties of other materials were considered. Three models (E3/1, E1/1, and E1/3) were analyzed with different values of the young's modulus of elasticity of the walls (E_{masonry}). The other material properties, including the unit weight of masonry (γ_{masonry}), Poisson's ratio of masonry (μ_{masonry}), unit weight of timber (γ_{timber}), young's modulus of elasticity of timber (E_{timber}), and Poisson's ratio of timber (μ_{timber}), were kept constant in this study which is summarized in Table 1. The base value of young's modulus of elasticity and Poisson's ratio was adopted from Adhikari & D'Ayala (2020) and the timber characteristics was adopted from IS 883 (1994).

Table 1: Material properties for different study models

Parameter	Value	Proportion of base value for each study models		
		E1/1	E3/1	E1/3
γ_{masonry}	22 KN/m ³ (Adhikari and D'Ayala, 2019)	1	1	1
E_{masonry}	240 MPa (Adhikari and D'Ayala, 2019)	1	3	1/3
μ_{masonry}	0.25	1	1	1
γ_{timber}	8.05 KN/m ³ (IS 883 : 1994 DESIGN OF STRUCTURAL TIMBER)	1	1	1
E_{timber}	12670 MPa (IS 883 : 1994 DESIGN OF STRUCTURAL TIMBER)	1	1	1
μ_{timber}	0.2	1	1	1

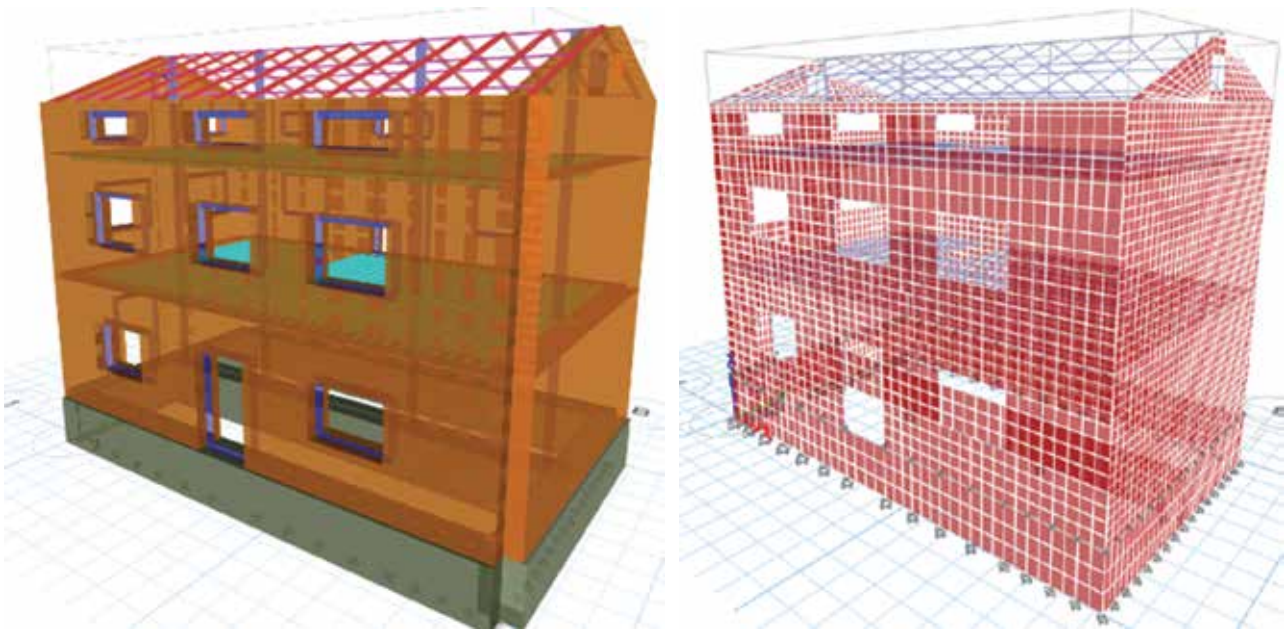


Figure 4: FEM model of the building

2.3 Analytical methods

Free vibration analysis of the structure was carried out using eigenvector analysis to identify the modal periods and frequencies. In order to determine the effect on modal results, the period of vibration corresponding to the highest mode for specified mass participation (40% and 70%) was determined that better represents the ranges of significant natural vibration periods of the building which in turn affects the seismic response of the building.

The effect of the change in wall elasticity to seismic loading has been carried out in terms of analysis of seismic base moment, building drift and deformation, and design forces and stresses in structural elements. Seismic loading is determined as per IS 1893 (Part1):2016 Indian Standard Criteria for Earthquake Resistant Design of Structures), lumped at mass or element location and seismic base moment is calculated at the base of the building as the sum of moment due to seismic forces acting from different height from the base. Both static method of analysis and response spectrum method of analysis was carried out for earthquake load determination, and response spectrum load was appropriately scaled to match the base shear in each case. As the response spectrum analysis better estimates the seismic load distribution in the structure considering the actual distribution of stiffness and mass in the system but it is customary to perform only static method of seismic analysis for low-rise buildings, the observed differences on base moments due to each case are compared. To the interest of this study, these differences in results are compared for each case of different wall elasticities. Further, as the load distribution differs due to different wall elasticities, the resulting building drift, forces and stresses in different structural elements also differ. These quantities are calculated from finite element analysis and their differences are evaluated.

3. Results and Discussion

The analysis was conducted for various types of structural responses namely, modal responses, seismic force distribution, deformation responses, and design stresses. These results are presented in the following subsections.

3.1 Modal responses

The dynamic analysis of the building was done through the modal analysis of the structure. Eigenvector analysis was done to determine the undamped free-vibration mode shapes and frequencies of the system upto the first 20 modes that provide an excellent insight into the behavior of the structure. Figure 5 presents the plot of the cumulative participating mass ratio against the natural vibration frequency of the buildings for three cases of E3/1, E1/1, and E1/3. As expected, the frequency of the structure increased with the increase in the elasticity of the wall material. However, it is interesting to note that as the elasticity decreases (E1/3 has minimum elasticity), the mass participation significantly increases in the initial modes, and negligibly more mass participation is achieved in the first 20 modes. Consequently, most of the mass participation was achieved in a smaller number of modes as the elasticity of the wall is lowered.

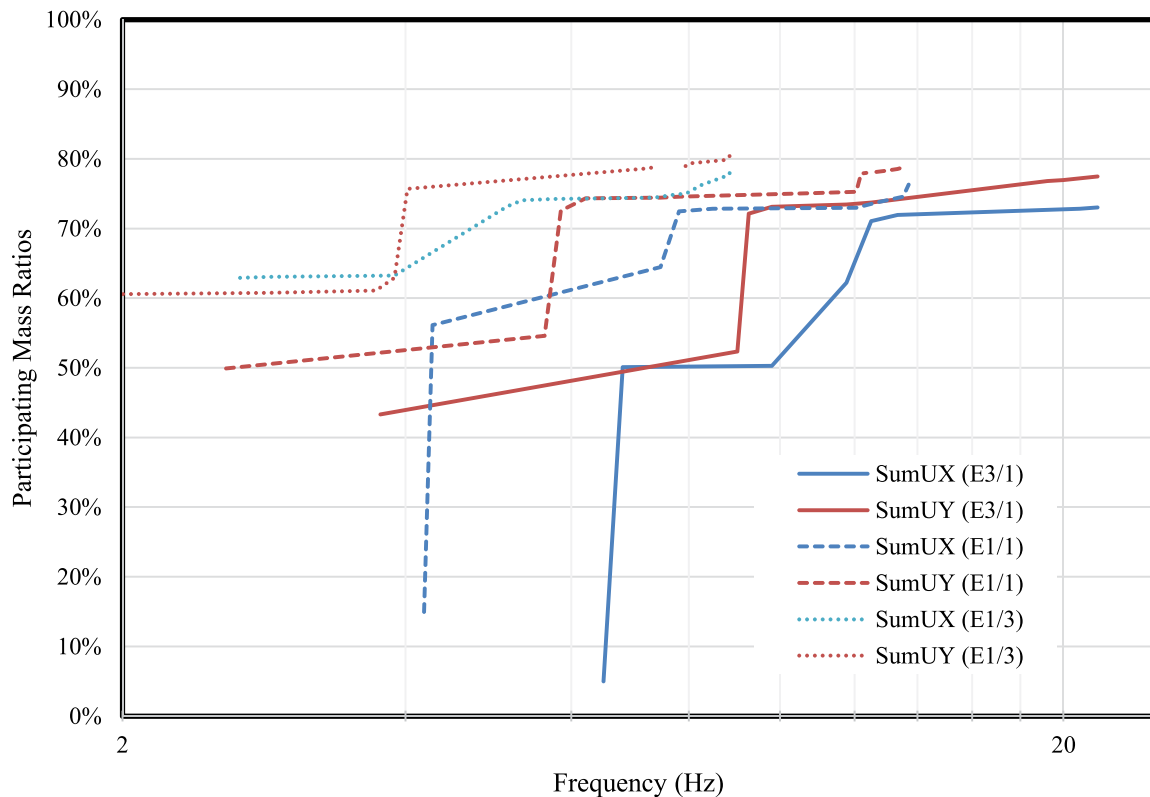


Figure 5: Modal shift of the structure for change in the elasticity of wall material

Similarly, Table 2 presents the period of vibration in seconds and its relative shift with respect to E1/1 base model. As the mass participation was distributed over a range of modes with different periods, for the maximum period of vibration at least 40% mass participation and 70% mass participation were considered. The data shows that when elasticity was increased by three times (E3/1), the period reduced by about 35% and when the elasticity was decreased by three times (E1/3), the period of vibration increased by about 35%. Although most of the design codes present constant design spectra for ranges of low-period buildings, the actual response of such buildings could be significantly different in actual earthquake depending on the dominant period of vibration of an earthquake. Hence, these differences in the period have no significant impact in the design earthquake force but its distribution in the building will be affected that can be predicted through dynamic analysis of the earthquake force.

Table 2: Shift in minimum period of vibration with respect to wall elasticity

Model	Cut-off at 40% Mass Participation				Cut-off at 70 % Mass Participation			
	T(x) sec	T(y) sec	D T(x)	D T(y)	T(x) sec	T(y) sec	D T(x)	D T(y)
E3/1	0.154	0.266	-34%	-31%	0.08	0.108	-38%	-37%
E1/1	0.234	0.388	100%	100%	0.128	0.171	0%	0%
E1/3	0.375	0.549	38%	29%	0.195	0.249	34%	31%

3.2 Seismic force distribution

The dynamic analysis of the building was also carried out using the response spectrum method for the determination of earthquake force distribution. The dynamic analysis was carried out using IS1893:2016 (IS 1893 (Part1):2016 Indian Standard Criteria for Earthquake Resistant Design of Structures, 2016) with the response spectrum curve for soft soil site that is representative for the Nepali cases. As the study focuses on identifying the extent of changes in the dynamic forces when there is the parametric change in material properties of the building, any of the typical response spectrum curves are expected to yield similar variations as far as low-rise masonry buildings are concerned. The seismic base shear in response spectrum analysis was scaled to match the results from the static earthquake analysis approach which was 1163 KN. Table 3 presents the change in the seismic base moment in response spectrum analysis compared to static analysis as well as the change in the seismic base moment in response spectrum analysis for various cases of wall elasticity compared to the base model. Table 3 shows that the static analysis significantly underestimates the base moment for masonry buildings by about 20% to 30% irrespective of the elasticity of the building. However, the base moment was only slightly affected by the elasticity of the building when the base-shear are scaled to the same value. Base moment was slightly increased by about 0.3% to 1.4% when the stiffness of wall increased by three times (model E3/1), and the base moment was slightly reduced by about 0.3 to 0.4% when the stiffness of wall decreased by three times (model E1/3).

Table 3: Base moments

Model	RS		Static		RS base moment compared to Static Moment		RS base moment compared to RS Base Model (E1/1)	
	Base Moment		Base Moment					
	Mx	My	Mx	My	D M(x)	D M(y)	D M(x)	D M(y)
E3/1	5530	6108	4694	4694	+12%	+30%	-0.4%	-0.2%
E1/1	5554	6120	4694	4694	+18%	+30%	0.0%	0.0%
E1/3	5630	6135	4694	4694	+20%	+31%	+1.4%	+0.3%

3.3 Building drift and deformation

The horizontal deflection of the building was determined as the maximum displacement of each floor under response spectrum earthquake loading. The displacement of different floor levels in each of the x-direction and y-direction due to seismic loading in the x-direction and y-direction respectively are presented in Figure 6 and Table 4.

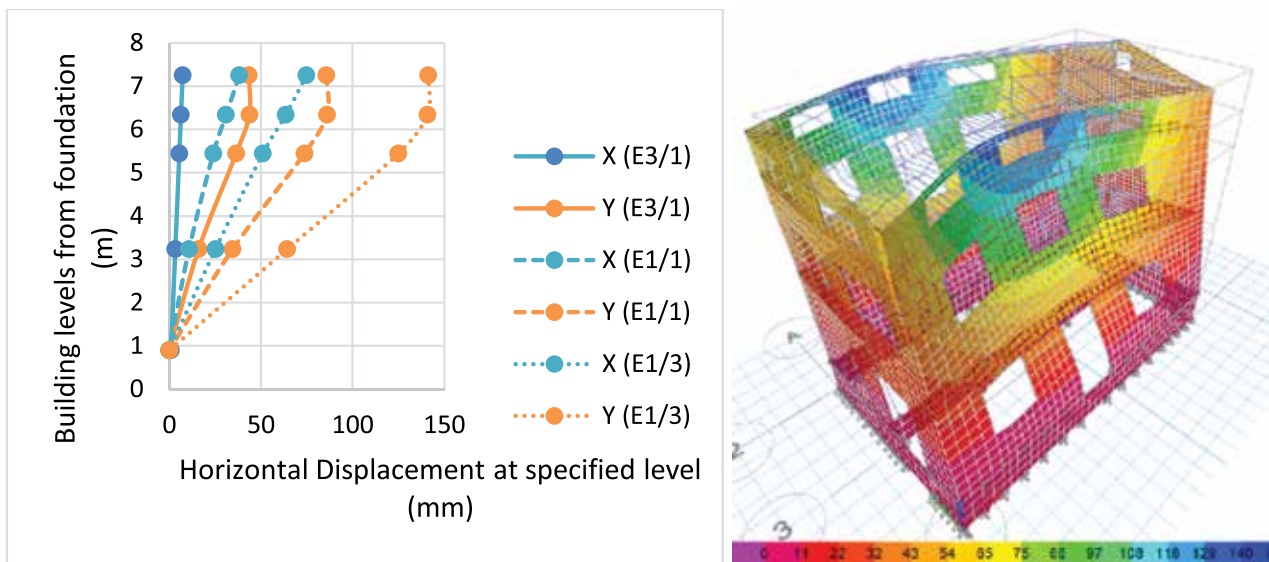


Figure 6: Building deformation for various models (left) and deformed shape in y-direction earthquake loading (right)

As the building is long in the x-direction, the y-direction lateral displacement is relatively more, with a maximum drift ratio of 2.76% at the ground floor and the average drift of the building being 2.22% for model E1/3. However, as shown in Figure 6, there is significant diaphragm deformation and the average drift ratio of the cross wall was only 0.79% at the eaves level corresponding to 50mm lateral deformation for the model E1/3.

Table 4: Horizontal displacement of building at different levels

Elevation	Horizontal displacement (mm) under corresponding seismic loading					
	X (E3/1)	Y (E3/1)	X (E1/1)	Y (E1/1)	X (E1/3)	Y (E1/3)
7.3	17.4	43.4	38.1	85.8	74.8	141.4
6.3	14.0	43.7	31.0	86.1	63.6	140.8
5.4	10.6	36.5	24.0	73.8	51.1	125.1
3.2	4.5	16.0	10.8	34.6	25.2	64.4
0.9	0.0	0.0	0.0	0.0	0.0	0.0

Table 5 presents the relative displacement of the building with different elasticity relative to the base model. As shown in the table, the analysis showed that the average lateral displacement decreased by 56% and 51% in the x and y direction respectively, when the wall elasticity increased by three times for model-E3/1 relative to model-E1/1. Similarly, the average lateral displacement increased by 112% and 71% in x and y directions respectively when the wall elasticity decreased by three times for model-E1/3 relative to model-E1/1.

Table 5: Relative horizontal displacement of building at different levels with respect to base model

Elevation	% Change in horizontal displacement compared to base model					
	X (E3/1)	Y (E3/1)	X (E1/1)	Y (E1/1)	X (E1/3)	Y (E1/3)
7.3	-54%	-49%	00%	00%	+96%	+65%
6.3	-55%	-49%	00%	00%	+105%	+64%
5.4	-56%	-50%	00%	00%	+113%	+70%
3.2	-59%	-54%	00%	00%	+134%	+86%
0.9	-	-	-	-	-	-
Average	-56%	-51%	00%	00%	+112%	+71%

3.4 Design forces and stresses

Design forces are calculated based on envelope values (most critical values) obtained from all the design load combinations. The design vertical compressive stress contours at the back façade wall and a side wall of the building are shown in Figure 7 and Figure 8 respectively.

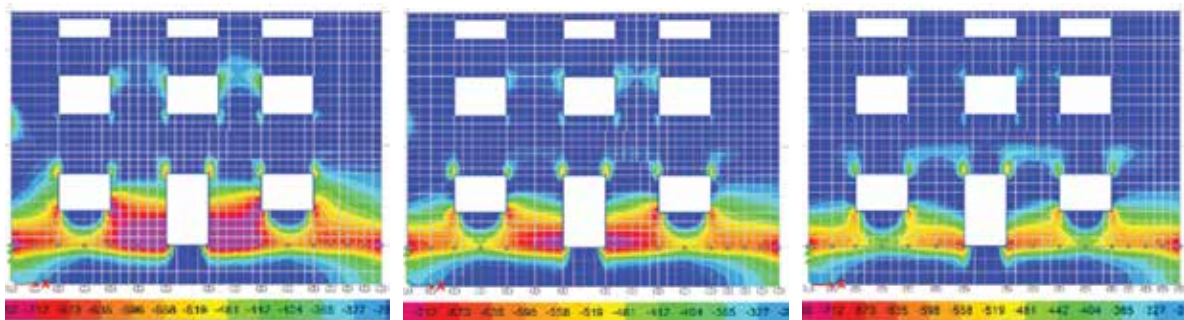


Figure 7: Design vertical compress stress (MPa) on back face of the building for models E3/1, E1/1, and E1/3 from left to right respectively

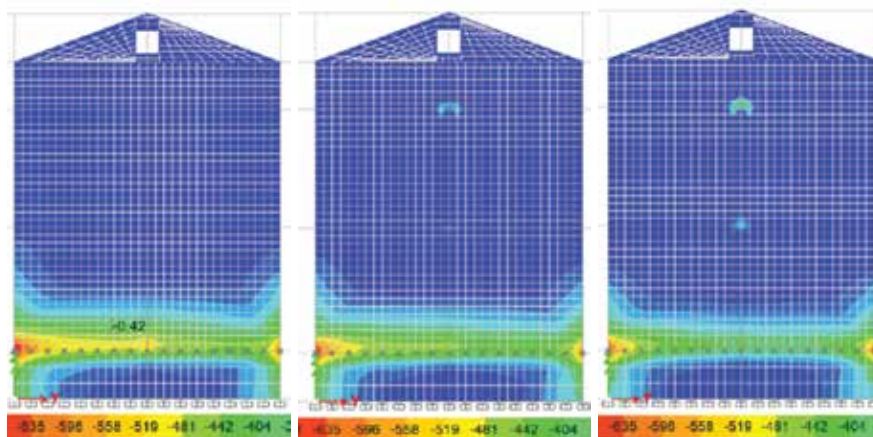


Figure 8: Design vertical compress stress (MPa) on a side face of the building for models E3/1, E1/1, and E1/3 from left to right respectively

Table 6: *The design forces in the second pier of back wall*

Model	Design Forces (KN)		% Variation	
	Compression	Shear	Compression	Shear
E3/1	-162.5	119.6	-2.3%	-2.4%
E1/1	-166.4	122.6	0.0%	0.0%
E1/3	-171.1	123.8	2.9%	1.0%

Figure 7 shows that the vertical compressive stresses concentrate more on ground floor walls in the E3/1 model significantly more than in the E1/3 model. However, Table 6 shows that the maximum design forces through the second pier of the back wall (as marked in Figure 7) is maximum for the E1/3 case. Although the variation is within 3%, it is interesting to note that the total force on any pier increases as the elasticity of the wall is reduced; however, the distribution of maximum stress is spread over a wider area in the wall with higher elasticity as shown in Figure 7.

4. Conclusions

The variation in dynamic characteristics of stone masonry buildings is perceived for a long time but barely quantified. This puts the analyses into a dilemma regarding the selection of material properties and their likely impact. To address the uncertainty encapsulated within material properties and its impact on dynamic characteristics and response of stone masonry, parametric analysis is performed considering the variation in elastic modulus. Finite element-based analysis highlight that the effects are more than what is being perceived, which prompts that the Codal provisions are too conservative to capture such fluctuations. Further, such fluctuations has pronounced effect on the dynamic response of the building. For instance, more mass participation was achieved in relatively smaller number of modes if the wall elasticity decreases and vice versa. Similarly, as the elasticity of wall was decreased, the period of vibration was increased as expected. In the studied typical residential masonry building, the time period varied by about 35% when the stiffness varied by three folds. Similarly, the base moment was slightly increased by about 0.3% to 1.4% when the stiffness of wall decreased by three times (model E1/3), and the base moment was slightly reduced by about 0.2 to 0.4% when the stiffness of wall increased by three times (model E3/1). More interestingly, although the base shear was matched in static and response spectrum methods for earthquake analysis, the base shear differed significantly. The base moment increased by about 18% and 30%, respectively, about x axis (along long direction) and about y axis (along short direction) of the building in the base model. The difference further increased for lower elasticity model (E1/3) to 20% while the difference decreased to 12% for higher elasticity model (E3/1) indicating that the base moment estimation differ significantly in dynamic analysis compared to static analysis even if the dynamic analysis is scaled to match the base shear. Similarly, the drift ratio significantly increased when the elasticity decreased. As the elastic modulus is increased by three times and decreased by three times, the peak displacement is decreased by about 50% and increased by about 100% which is instrumental to note that the type and quality of stone masonry can easily lead to such fluctuations. The results presented in this study could provide insights to further quantify the effects of uncertainties in material characteristics. Further studies in terms of the rock type compliant variations and their effects in dynamic response are prompted by the results of this study.

Acknowledgments

The authors acknowledge University Grants Commission (UGC) for partially funding this research work under grant number "UGC Grant Award No. FRG/74_75/Engg-5".

Declaration of Competing Interest

The authors declare that they have no known competing financial interests or personal relationships that could have appeared to influence the work reported in this paper.

References

- Adhikari, R., & Gautam, D. (2019). Component level seismic fragility functions and damage probability matrices for Nepali school buildings. *Soil Dynamics and Earthquake Engineering*, 120. <https://doi.org/10.1016/j.soildyn.2019.02.009>
- Adhikari, R., Jha, P., Gautam, D., & Fabbrocino, G. (2019). Seismic strengthening of the Bagh Durbar heritage building in Kathmandu following the Gorkha earthquake sequence. *Buildings*, 9(5). <https://doi.org/10.3390/buildings9050128>
- Adhikari, R. K., & D'Ayala, D. (2020). 2015 Nepal earthquake: seismic performance and post-earthquake reconstruction of stone in mud mortar masonry buildings. In *Bulletin of Earthquake Engineering* (Vol. 18, Issue 8). Springer Netherlands. <https://doi.org/10.1007/s10518-020-00834-y>
- Adhikari, R., Rupakhety, R., Giri, P., Baruwal, R., Subedi, R., Gautam, R., & Gautam, D. (2022). Seismic Fragility Analysis of Low-Rise RC Buildings with Brick Infills in High Seismic Region with Alluvial Deposits. *Buildings*, 12(1). <https://doi.org/10.3390/buildings12010072>
- Ahmad, N., Ali, Q., Ashraf, M., Alam, B., & Naeem, A. (2012). Seismic vulnerability of the Himalayan half-dressed rubble stone masonry structures, experimental and analytical studies. *Natural Hazards and Earth System Sciences*, 12(11). <https://doi.org/10.5194/nhess-12-3441-2012>
- IS 1893 (Part1):2016 Indian Standard Criteria for Earthquake Resistant Design of Structures, (2016).
- Chettri, N., Gautam, D., & Rupakhety, R. (2021a). Seismic Vulnerability of Vernacular Residential Buildings in Bhutan. *Journal of Earthquake Engineering*. <https://doi.org/10.1080/13632469.2020.1868362>
- Chettri, N., Gautam, D., & Rupakhety, R. (2021b). From Tship Chim to Pa Chim: Seismic vulnerability and strengthening of Bhutanese vernacular buildings. *Masonry Construction in Active Seismic Regions*, 253–288. <https://doi.org/10.1016/B978-0-12-821087-1.00009-0> Computers and Structures Inc. (2020). *ETABS*.
- NBC-105:2020 Nepal National Building Code for Seismic Design of Buildings in Nepal, (2020).
- Gautam, D. (2018). Observational fragility functions for residential stone masonry buildings in Nepal. *Bulletin of Earthquake Engineering* 2018 16:10, 16(10), 4661–4673. <https://doi.org/10.1007/S10518-018-0372-2>
- Gautam, D., Adhikari, R., Rupakhety, R., & Koirala, P. (2020). An empirical method for seismic vulnerability assessment of Nepali school buildings. *Bulletin of Earthquake Engineering*, 18(13), 5965–5982. <https://doi.org/10.1007/s10518-020-00922-z>
- Gautam, D., & Chaulagain, H. (2016). Structural performance and associated lessons to be learned from world earthquakes in Nepal after 25 April 2015 ($M < \infty > W < / \infty > 7.8$) Gorkha earthquake. *Engineering Failure Analysis*, 68. <https://doi.org/10.1016/j.engfailanal.2016.06.002>
- Gautam, D., Chettri, N., Tempa, K., Rodrigues, H., & Rupakhety, R. (2022). Seismic vulnerability of Bhutanese vernacular stone masonry buildings: From damage observation to fragility analysis. *Soil Dynamics and Earthquake Engineering*.
- Gautam, D., Fabbrocino, G., & Santucci de Magistris, F. (2018). Derive empirical fragility functions for Nepali residential buildings. *Engineering Structures*. <https://doi.org/10.1016/j.engstruct.2018.06.018>
- Gautam, D., Rodrigues, H., Bhetwal, K. K., Neupane, P., & Sanada, Y. (2016). Common structural and construction deficiencies of Nepalese buildings. *Innovative Infrastructure Solutions*, 1(1). <https://doi.org/10.1007/s41062-016-0001-3>
- Gautam, D., Rupakhety, R., Adhikari, R., Shrestha, B. C., Baruwal, R., & Bhatt, L. (2021). Seismic vulnerability of Himalayan stone masonry: Regional perspectives. *Masonry Construction in Active Seismic Regions*, 25–60. <https://doi.org/10.1016/B978-0-12-821087-1.00014-4>
- IS 883. (1994). *Design of Structural Timber In Building -Code of Practice*. Bureau of Indian Standards.
- Parajuli, R. R. (2021). Features and seismic response of large masonry structures: A case study of Singh Durbar main building, Nepal. In *Masonry Construction in Active Seismic Regions*. <https://doi.org/10.1016/b978-0-12-821087-1.00013-2>
- Parajuli, R. R., Furukawa, A., & Gautam, D. (2020). Experimental characterization of monumental brick masonry in Nepal. *Structures*, 28. <https://doi.org/10.1016/j.istruc.2020.09.065>
- Parajuli, R. R., & Kiyono, J. (2015). Ground motion characteristics of the 2015 Gorkha earthquake, survey of damage to stone masonry structures and structural field tests. *Frontiers in Built Environment*, 1. <https://doi.org/10.3389/fbuil.2015.00023>
- Varum, H., Dumar, R., Furtado, A., Barbosa, A. R., Gautam, D., & Rodrigues, H. (2018). Seismic performance of buildings in Nepal after the Gorkha earthquake. In *Impacts and Insights of the Gorkha Earthquake*. <https://doi.org/10.1016/B978-0-12-812808-4.00003-1>